

A REAL-TIME PROCESSING METHOD BASED ON RANDOM SAMPLING AND COMPRESSIVE SENSING FOR INERTIAL SENSOR SIGNAL

XINGGUO JIANG^{1,2}, ZHENZHEN LUO², HAIYOU LI^{1,2} AND FABI ZHANG^{1,2}

¹Guangxi Key Laboratory of Precision Navigation Technology and Application

²School of Information and Communication

Guilin University of Electronic Technology

No. 1, Jinji Road, Qixing District, Guilin 541004, P. R. China

tonny-jiang@guet.edu.cn

Received December 2016; accepted March 2017

ABSTRACT. *In this paper, a real-time processing method for inertial sensor signal is proposed based on the random sampling and compressive sensing theory. Firstly, the inertial sensor signal is sampled by random sampling to reduce the number of sampling data. And then the original signal is reconstructed by a few of measurement values. The results validate that the signal-to-noise ratio of dynamic signal can be improved by about 7.15 dB with only 20% of the sampling data, and the zero-drift value of static signal also can be reduced greatly. Matlab/Simulink platform is used to further verify the feasibility of the provided method, in which the real-time processing can be realized. The presented method can provide a significant reference for the real-time processing of inertial sensor signal in terrible environments where it is hard to obtain the effective sampling data of signal.*

Keywords: Inertial sensor, Random sampling, Compressive sensing, Real-time processing

1. Introduction. Inertial navigation technology [1] is widely used in military and civil fields. Inertial sensor [2,3] is a core component of the inertial navigation system. However, the precision of inertial sensor signal is greatly affected by random noises. With the development of technology, the demand of precision is getting higher and higher. The method to improve the precision has attracted much attention during these years.

Filtering is one of methods to improve the precision of inertial sensor signal. Lai et al. [4] used Fourier transform to process signal for improving the precision of signal. However, it is not suitable for random noises. Stebler et al. [5] have applied Wavelet filtering to inertial navigation, which can effectively reduce random noises. However, Wavelet filtering needs complex computation. Compressed Sensing (CS) [6,7] is an emerging theory that has attracted considerable research interest. In CS theory, for the sparse signal, noises can be eliminated without the loss of the useful signal. For example, Lei et al. [8] proposed self-adaptive sparse representation to process the flutter signal. The processing effect is better and there is no need to set up a model in this method, but the number of sampling data is still larger. Random sampling [9], as a supplement to traditional sampling method, provides a solution to reconstruct signal with less sampling data.

To reduce random noises, in this paper random sampling and CS theory are combined to realize the real-time processing of inertial sensor signal. Compared with traditional algorithms, the proposed method can significantly improve the precision of inertial sensor signal. The rest of this paper is organized as follows. Section 2 introduces the CS theory. The method of real-time processing is described in Section 3 followed by the experiments and results in Section 4. Then conclusions are presented in Section 5.

- (1) Determine the optimal sampling interval of k from the uniform sampling;
- (2) Determine \mathbf{D} with k as the maximum interval in non-uniform sampling;
- (3) The inertial sensor signal is measured by Φ to obtain the measurement values \mathbf{Y} ;
- (4) Reconstruct the original signal \mathbf{S} from the measurement values \mathbf{Y} .

3.2. Real-time processing. In real-time processing, the original signal needs to be input point by point, and also in this manner, the reconstructed signal is output. When the signal with the length of m is processed, the corresponding reconstructed signal can be described as $\hat{\mathbf{s}}(1), \hat{\mathbf{s}}(2), \hat{\mathbf{s}}(3), \dots, \hat{\mathbf{s}}(m)$, where $\hat{\mathbf{s}}(m)$ is the value of real-time processing at time $t = m$. When the next signal point $\mathbf{s}(m + 1)$ arrives, the value $\mathbf{s}(1)$ is abandoned, and $\hat{\mathbf{s}}(m + 1)$ becomes the output value at time $t = m + 1$, and so on. In addition, to meet the requirement of real-time processing, the length of processing signal should be short as possible. The results validate the real-time processing can be realized with the length of 32 in each segment. The method can be described as the following:

- a) Pre-store sampling data with the length of m in original signal \mathbf{S} ;
- b) Obtain the measurement values by Φ , and from them the signal $\hat{\mathbf{S}}$ is reconstructed;
- c) Output the reconstructed signal point $\hat{\mathbf{s}}(m)$;
- d) Input signal point $\mathbf{s}(m + 1)$, shift backward a point, and then the value $\mathbf{s}(1)$ is abandoned.

Repeat steps from b) to d).

3.3. Parameters determination. Core parameters of Ψ , Φ , and k can be determined by comparisons. The frequency above 500 Hz of inertial sensor signal is taken as noises, and it is superimposed on a sinusoidal signal with the frequency of 100 Hz. The sampling frequency of superimposed signal is 5000 Hz and SNR is 4.49 dB. For better observation, Figures 2, 3, 4 only show 100 signal points.

Ψ can be selected from typical sparse basis of Fourier basis, Cosine basis and Wavelet basis. Figure 2 shows the effects of different sparse bases. Wavelet basis is more suitable for non-stationary or mutated signal, while the inertial sensor signal is relatively stationary. With the Fourier basis, the signal is sparser and the processing effect is the best in three bases. Therefore, the Fourier basis is best suitable for the inertial sensor signal.

For the measurement matrix Φ , there are common matrices as Gauss matrix, Bernoulli matrix and Topolitz matrix. Figure 3 shows the effects of processing. There is no significant difference between the three. However, compared with the other two matrices,

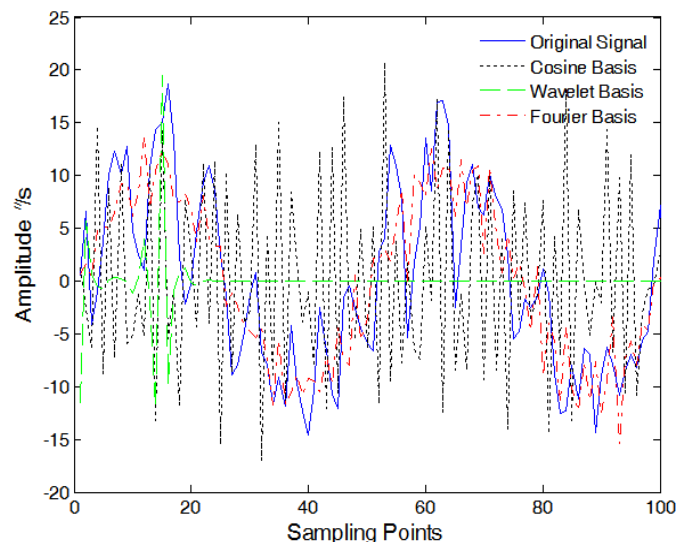


FIGURE 2. Effects of different sparse bases

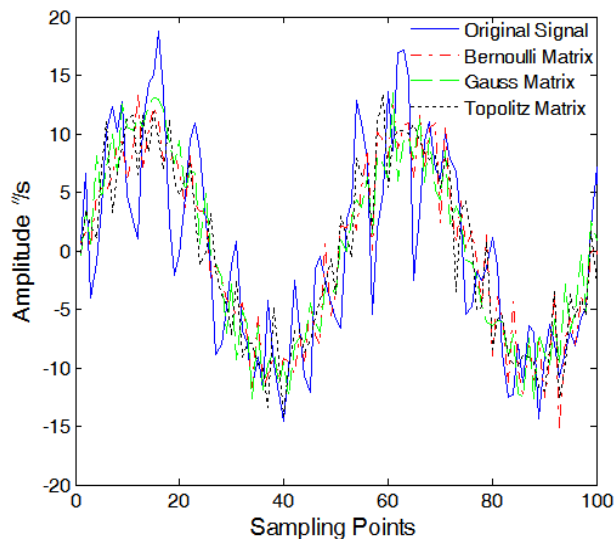


FIGURE 3. Effects of different measurement matrices

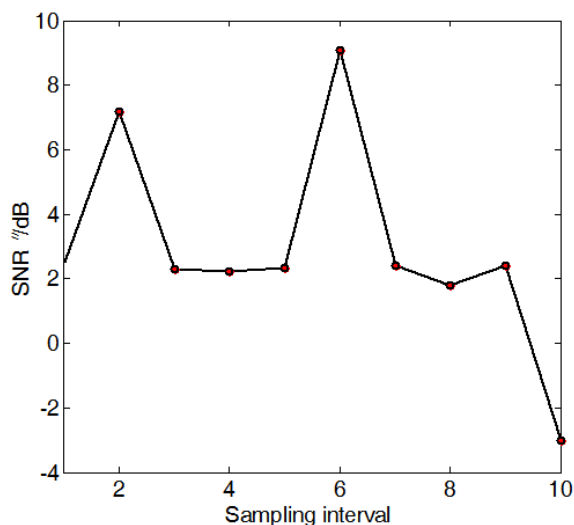


FIGURE 4. SNR of the reconstructed signal

Topolitz matrix is composed by simple ± 1 elements, which greatly reduces the storage space and is easy to implement with hardware. So Topolitz matrix is more suitable for the inertial sensor signal.

The optimal sampling interval k is determined by uniform sampling. SNR of the reconstructed signal from different sampling intervals is shown in Figure 4. As sampling interval increases, the sampling frequency of signal decreases. Since the frequency of noises is over 500 Hz, with the sampling frequency lower than 1000 Hz, noises can hardly be reconstructed while the signal can be reconstructed. As shown in Figure 4, the optimal sampling interval is 6, and then the signal can be non-uniform sampled with the sampling interval less than or equal to 6.

The reconstruction algorithm mainly includes Basis tracking [10] and Greedy tracking [11] in CS theory. With faster speed, the Greedy tracking, such as Orthogonal Matching Pursuit (OMP), can be used as the reconstruction algorithm for the inertial sensor signal.

4. Experiments and Results.

4.1. Simulation verification. To verify the feasibility of the provided method, the frequency above 500 Hz of inertial sensor signal is taken as noises, and then it is superimposed on a sinusoidal signal with the frequency of 50 Hz. The superimposed signal is used as dynamic signal for experiments, with the sampling frequency of 5000 Hz and the length $N = 300$. The processing effect can be evaluated by SNR, mean square error and the maximum phase shift. Mean square error refers to the expected value that is the square of difference between real signal and reconstructed signal, which measures the average error. Maximum phase shift refers to the phase difference that can be used to evaluate the navigation performance.

Figure 5 shows SNR of the reconstructed signal from non-uniform sampling. The data indicate that SNR increases with the increasing of sampling proportion. When the sampling data increases from 15% to 20%, SNR increases at the fastest speed. Since sinusoidal signal is periodic with some regularity, it can be reconstructed with the certain number of sampling data. Therefore, as the sampling data increases from 30% to 70%, SNR increases slower relatively and tends to be stable gradually, namely the sampling data is enough to reconstruct the signal. Even with only 15% of the sampling data, SNR of the reconstructed signal can still increase by 5.32 dB. Figure 6 shows the processing effects

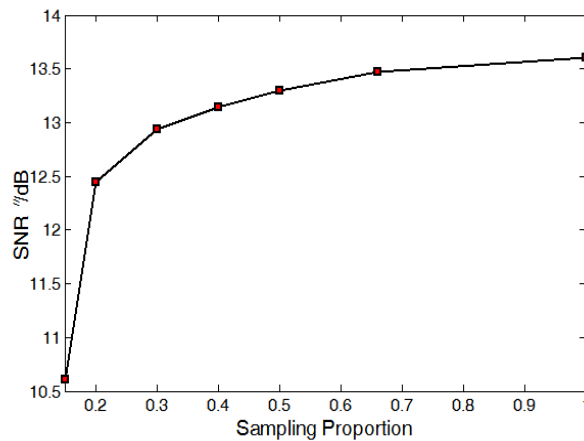


FIGURE 5. SNR of reconstructed signal for dynamic signal

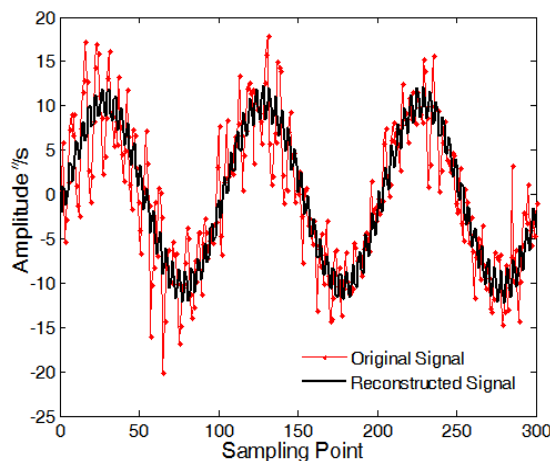


FIGURE 6. Effects with 20% of the sampling data for dynamic signal

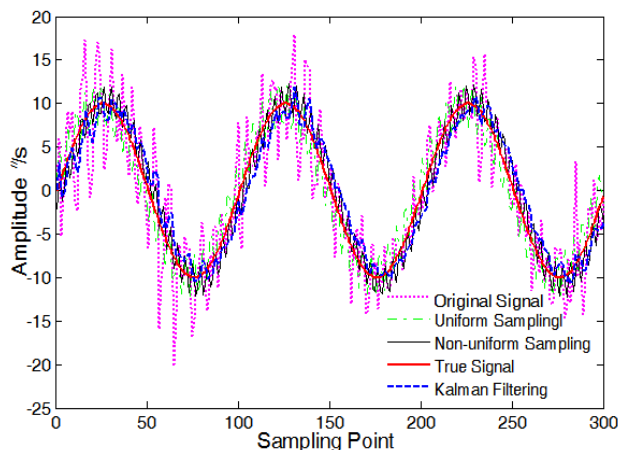


FIGURE 7. Effects of different methods for dynamic signal

TABLE 1. The performance comparisons for dynamic signal

performance parameters	SNR /dB	mean square error /($''/s$)	maximum phase shift / $^{\circ}$
original signal	5.29	14.778 9	\
uniform sampling	10.9	3.950 9	16.71
66% of the sampling data	13.47	2.154 1	12.59
50% of the sampling data	13.30	2.320 2	12.62
40% of the sampling data	13.14	2.361 6	12.68
30% of the sampling data	12.95	2.534 6	13.12
20% of the sampling data	12.44	2.875 6	13.43
15% of the sampling data	10.61	4.423 0	16.45
Kalman filtering	12.96	2.534 8	13.10

with 20% of the sampling data. Compared with the original signal, SNR increases by 7.15 dB; the mean square error decreases by 11.903 3($''/s$); the phase shift lags behind 12.59 $^{\circ}$.

Figure 7 shows the comparison of effects between the presented method and Kalman [12], with the same experimental environment and signal. The uniform sampling indicates sampling with the optimal sampling interval of 6, and the non-uniform sampling indicates sampling with 20% of data. The comparisons of performance between two methods are recorded in Table 1. With the 66% of the sampling data, SNR of the reconstructed signal increases by 8.18 dB; the mean square error decreases by 12.624 8($''/s$); the phase shift lags behind 12.59 $^{\circ}$. Therefore, the results validate that the presented method can effectively reduce the noises and improve the processing performance.

The static signal of inertial sensor is used to verify the proposed method further. The actual static signal is sampled from some Fiber Optic Gyro (FOG), with the sampling frequency of 5000 Hz and the length $N = 300$. Zero-drift value, one of the main errors for static signal, refers to the output value of signal while its input is zero. Moreover, to compare and evaluate the effects, the reconstructed signal by wavelet is selected as a reference of real signal.

Figure 8 shows SNR of the reconstructed signal from non-uniform sampling. The varying tendency is the same as Figure 5. Namely, SNR increases at the fastest speed before the critical point, and then it increases relatively slower. Figure 9 shows the effects with 20% of the sampling data. Compared with the original signal, SNR of the reconstructed signal increases by 5.9 dB; the mean square error decreases by 1.090 9e-06($''/s$); the zero-drift value reaches 6.274 1e-04($''/s$); the phase shift lags behind 30.69 $^{\circ}$.

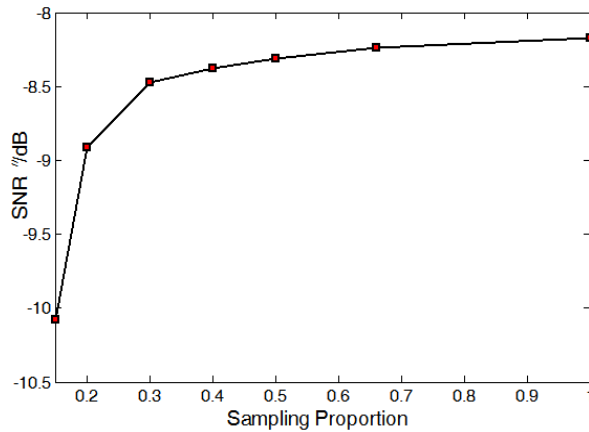


FIGURE 8. SNR of reconstructed signal for static signal

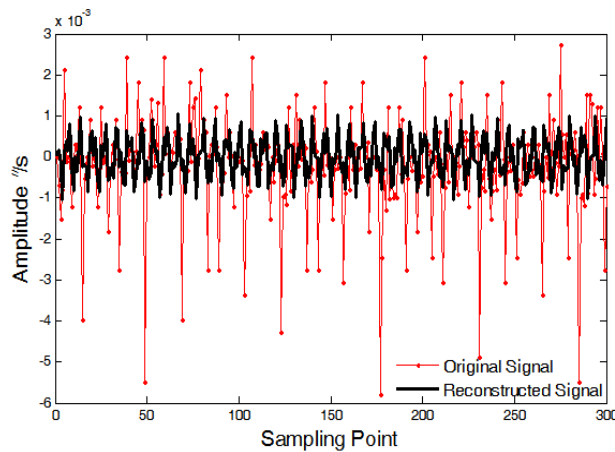


FIGURE 9. Effects with 20% of the sampling data for static signal

TABLE 2. The performance comparisons for static signal

performance parameters	SNR /dB	mean square error /(" /s)	zero-drift value /(" /s)	maximum phase shift /°
original signal	-14.81	1.483 7e-06	0.001 2	\
uniform sampling	-8.33	3.382 1e-07	5.153 4e-04	28.91
66% of the sampling data	-8.24	3.253 6e-07	4.749 1e-04	28.63
50% of the sampling data	-8.31	3.358 7e-07	4.918 3e-04	28.88
40% of the sampling data	-8.38	3.413 6e-07	5.357 4e-04	28.94
30% of the sampling data	-8.47	3.464 4e-07	5.584 4e-04	29.12
20% of the sampling data	-8.91	3.928 0e-07	5.725 9e-04	30.69
15% of the sampling data	-10.08	4.879 6e-07	6.235 3e-04	32.12
Kalman filtering	-7.29	2.623 7e-07	5.802 3e-04	27.26

Figure 10 shows the comparison with Kalman. The results are recorded in Table 2. With the 66% of the sampling data, SNR of the reconstructed signal increases by 6.57dB; the mean square error and zero-drift value decrease by 1.1583 4e-06(" /s), 7.250 9e-04(" /s) respectively; the phase shift lags behind 28.88°. Therefore, the results validate that the proposed method is also effective for the static signal.

Kalman has better effect on inertial sensor signals, but it needs to build model in advance and higher sampling rate. The proposed method can greatly reduce the sampling

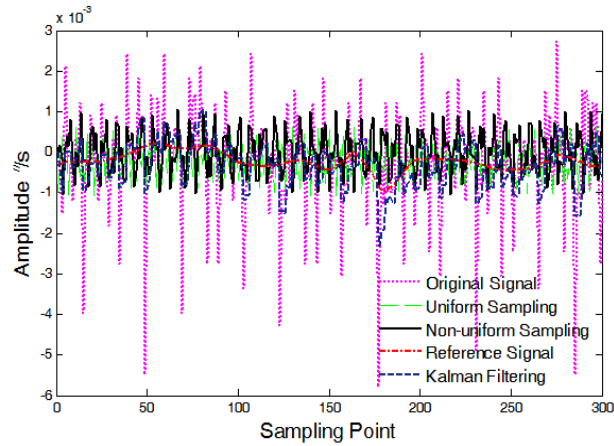


FIGURE 10. Effects of different methods for static signal

data with random sampling and shorten the processing time, which is beneficial for the real-time processing.

4.2. Simulink platform. Simulink platform is used to further verify the practical application of the method. The module can be built to simulate the DSP running mode. As a user-defined module, s-function can be called repeatedly by Simulink in each time interval of T_S , which implements a virtual clock. In this way, the core operating characteristic of simulation system keeps consistent with DSP in some actual system. When simulation starts from the origin, the s-function is executed each T_S second. This way is similar with the execution mode of DSP interrupt. The sampling frequency of the inertial sensor signal is 5000 Hz, and then T_S is set as 0.2 ms. Simulation platform is shown as Figure 11.

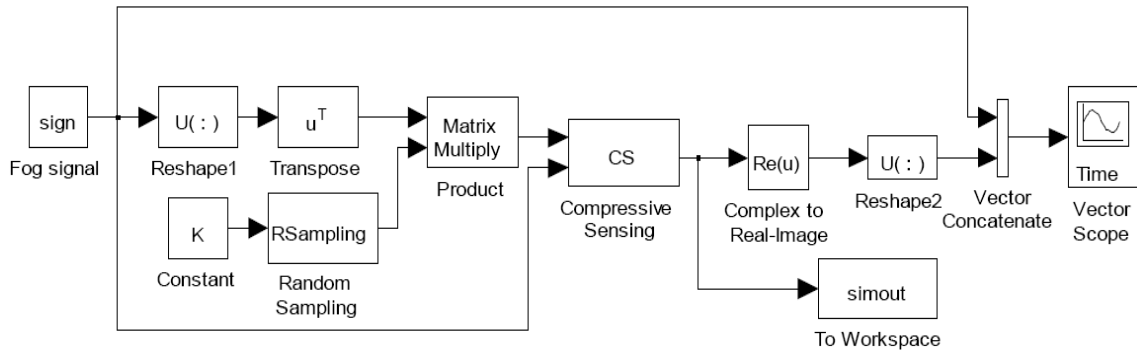


FIGURE 11. Simulink platform

In Figure 11, both RSampling and CS are built with s-function modules, which are used to realize the processing of Random Sampling and Compressive Sensing respectively. The sign module is defined to input FOG signal and deposit firstly the actual sampling data with the length of 32. The constant k refers to the maximum sampling interval in uniform sampling. And then the result of processing in vector scope is shown in Figure 12.

In Figure 12, the CH 1 refers to the original inertial sensor signal that contains noises. The CH 2 refers to the reconstructed signal. As seen in Figure 12, noises can be reduced significantly. In the Simulink platform, it takes $113 \mu s$ to realize the processing for each signal point, which is lower than the sampling interval $200 \mu s$. Therefore, the proposed method realizes real-time processing for the inertial sensor signal.

5. Conclusions. In this paper, based on random sampling and CS theory, the presented method realizes the real-time processing with less sampling data and also has certain versatility. This is significant for inertial sensor signal in the extremely terrible environment

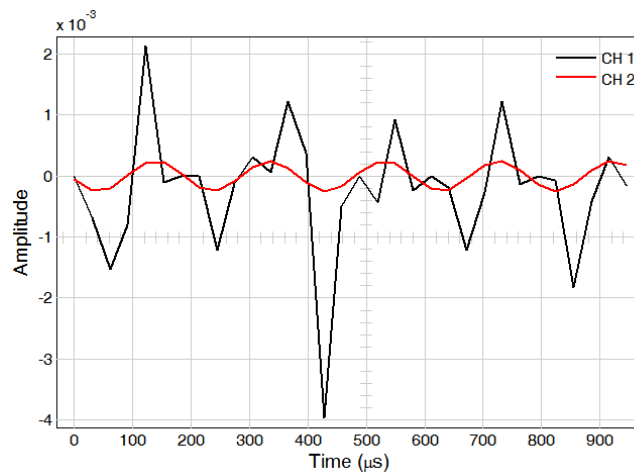


FIGURE 12. Signal processing effect on Simulink platform

where there are lots of interferences. Moreover, considering the limitation of common parameters in signal processing, some self-adaptive parameters can be introduced to improve further the effect of processing in the future.

Acknowledgment. This work is mainly supported by Guangxi Key Laboratory of Precision Navigation Technology and Application, Guilin University of Electronic Technology (No. DH201507).

REFERENCES

- [1] P. G. Savage, Blazing gyros: The evolution of strapdown inertial navigation technology for aircraft, *Journal of Guidance, Control, and Dynamics*, vol.36, no.3, pp.637-655, 2013.
- [2] A. Rampp, J. Barth, S. Schüle et al., Inertial sensor-based stride parameter calculation from gait sequences in geriatric patients, *IEEE Trans. Biomedical Engineering*, vol.62, no.4, pp.1089-1097, 2015.
- [3] D. K. Shaeffer, MEMS inertial sensors: A tutorial overview, *IEEE Communications Magazine*, vol.51, no.4, pp.100-109, 2013.
- [4] D. T. H. Lai, R. Begg, E. Charry and M. Palaniswami, Frequency analysis of inertial sensor data for measuring toe clearance, *IEEE International Conference on Intelligent Sensors, Sensor Networks and Information Processing*, pp.303-308, 2008.
- [5] Y. Stebler, S. Guerrier, J. Skaloud and M. P. Victoria-Feser, Generalized method of wavelet moments for inertial navigation filter design, *IEEE Trans. Aerospace and Electronic Systems*, vol.50, no.3, pp.2269-2283, 2014.
- [6] S. Qaisar, R. M. Bilal, W. Iqbal et al., Compressive sensing: From theory to applications, a survey, *Journal of Communications and Networks*, vol.15, no.5, pp.443-456, 2013.
- [7] B. Bougher, Introduction to compressed sensing, *The Leading Edge*, vol.34, no.10, pp.1256-1257, 2015.
- [8] J. Lei, X. Meng and Z. Xiang, Flutter signal extracting technique based on FOG and self-adaptive sparse representation algorithm, *Proc. of SPIE*, vol.101581, 2016.
- [9] M. Fischetti, A. Lodi, M. Monaci et al., Improving branch-and-cut performance by random sampling, *Mathematical Programming Computation*, vol.8, no.1, pp.113-132, 2016.
- [10] M. A. Khajehnejad, W. Xu, A. S. Avestimehr and B. Hassibi, Improving the thresholds of sparse recovery: An analysis of a two-step reweighted basis pursuit algorithm, *IEEE Trans. Information Theory*, vol.61, no.9, pp.5116-5128, 2015.
- [11] D. Sundman, S. Chatterjee and M. Skoglund, Greedy pursuits for compressed sensing of jointly sparse signals, *The 19th European Signal Processing Conference*, pp.368-372, 2011.
- [12] R. Peesapati, S. L. Sabat, K. P. Karthik et al., Efficient hybrid Kalman filter for denoising fiber optic gyroscope signal, *Optik – International Journal for Light and Electron Optics*, vol.124, no.20, pp.4549-4556, 2013.